A rhenium(I) complex which reacts with aldehydes and ketones in aqueous media: a structural, spectroscopic and theoretical analysis.

Lindsay P. Harding[a], Asuka A.T. McRobbie[a], T. Riis-Johannessen[b], Simon J.A. Pope[c], Craig R. Rice[a], Donna Rollinson[a], and Martina Whitehead[a*]

[a] Department of Chemical and Biological Sciences, University of Huddersfield, Huddersfield HD1 3DH. Fax: (+44) 148-447-2182; Tel: (+44) 148-447-3759; E-mail: m.whitehead@hud.ac.uk

[b] School of Chemistry, Cantock's Close, University of Bristol, BS8 1TS.

[c] School of Chemistry, Main Building, Cardiff University, Cardiff CF10 3AT. Fax: (+44) 292-087-4030; Tel (+44) 292-087-9316.

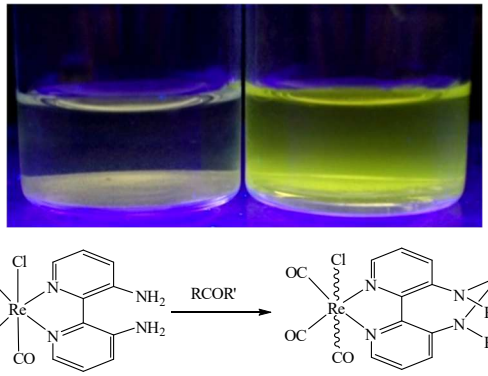

Abstract.

A Re(I) complex of 3,3'-diamino-2,2'-bipyridine reacts irreversibly with aldehydes and unhindered ketones in water to form bis-aminal cyclised derivatives with the solid-state structure of the reaction with benzaldehyde reported. This reaction produces a Re(I) complex which is significantly more emissive than the starting compound.

Introduction.

In recent years transition metal complexes have been utilised as sensors or probes for volatile organic compounds (VOCs). Such systems have generally been limited to solid state arrays of either Pt(II),[1-10] Ag(I) or Au(I)[11-13] complexes where intermolecular metal-metal interactions form the basis of the signalling response, be it either colourimetric and/or emissive. Consequently, the reversible sorption of the VOC into the lattice of the complexes modulates the metal-metal interactions inducing a change in colour or luminescence output. The nature of some of these species has allowed thin films to be applied to optical fibres allowing transduction of the optical response of selected vapochromic materials.[14,15] The aim of this investigation was to access a responsive metal-based molecule which possesses reactivity to simple organic compounds in the solution state, preferably aqueous media. Herein we report a Re(I) complex which differentially reacts with both aldehydes and unhindered ketones in aqueous media, which in the process dramatically modulates both the UV-visible absorption properties and the luminescence characteristics.

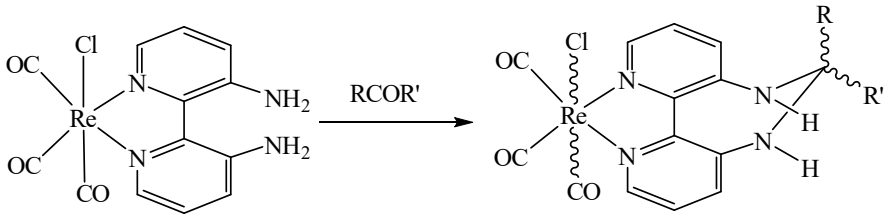

Scheme 1 Aminal derivatives of compound **1**. **2a** R = CH_3- and R' = H, **2b** R = 4-$O_2NC_6H_5$- and R' = H, **2c** R = R' = CH_3- and **2d** R = Ph and R' = H.

Results and Discussion.

The rhenium-containing complex 1 was prepared by heating 3,3-diamino-2,2'-bipyridine[16] with $[ReCl(CO)_5]$ in $CHCl_3$ to reflux and after filtration, pure **1** was obtained as a pale yellow powder. This complex reacts readily and irreversibly with acetaldehyde to give the corresponding cyclized species **2a**, where the aldehyde has added across the diamine unit, with the loss of water, to give the 7-membered diaza macrocycle. Whilst the complex **1** readily reacts with acetaldehyde no reaction with either aromatic aldehydes or ketones was observed under the same conditions. However, reaction with 4-nitrobenzaldehyde, acetone and benzaldehyde occurs virtually instantaneously upon addition of a catalytic amount of acid, to give **2b**, **2c** and **2d** respectively, although even under these conditions no reaction with 4-bromoacetophenone was observed (Scheme 1).

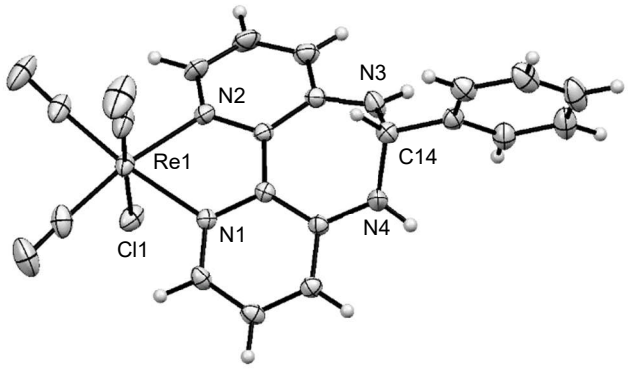

Fig. 1 Molecular structure of **2d** (anisotropic displacement parameters are shown at a 50 % probability level). Selected bond lengths: Re(1)-C(1) 1.913(3), Re(1)-C(3) 1.919(3), Re(1)-C(2) 1.920(3), Re(1)-N(2) 2.148(2), Re(1)-N(1) 2.160(2) and Re(1)-Cl(1) 2.5048(6) Å.

The X-ray single crystal structure of the reaction product formed with benzaldehyde was obtained (Fig. 1).[17] As would be expected the structure shows the 3,3'-diamino-2,2'-bipyridine unit coordinated to the rhenium centre via the bipyridine nitrogen atoms. The aldehyde has added across the 3,3'-diamino unit such that the benzaldehyde moiety lies in the equatorial plane of the bipyridine ring system.[18-20] Analysis of the isolated crystalline material by ^{1}H NMR shows double the amount of signals that would be expected for the complex **2d** with one set of signals attributable to a minor component (~30%). Correspondingly, there are four possible isomers formed upon reaction with benzaldehyde (Fig. 2) with the phenyl unit reacting to give the equatorial or axial isomers (Fig 2i and 2ii). This is

coupled with potential conformers of i and ii which are formed dependent upon the relative position of the axial chloride ligand (e.g. adopting a *cis*- or *trans*-oid conformation with respect to the axial chloride ligand iii and iv). The concentration of one of the isomers in the ^{1}H NMR of **2d** is a product of selective crystallisation in the isolation process as in the ^{1}H NMR of **2b** equal amounts of both isomers are observed. Heating a sample of **3b** in $(CD_3)_2SO$ (298 – 353 K) does result in altering the ^{1}H NMR spectrum, with both a change in the chemical shift and multiplicity of selected signals, but the spectrum still contains signals corresponding to two isomers. It seems only reasonable to assume that this change in the ^{1}H NMR upon heating is due to ring flipping of the animal ring and it will interconvert isomers i – iv and ii – iii. However, as two isomers are still present at this elevated temperature it seems highly like that the two isomers arise from the *cis*- or *trans*-oid conformation of the 4-nitrophenyl substituent with respect to the axial chloride. Cooling the sample back to room temperature returns the spectrum to its original chemical shift and multiplicity discounting any heat induced chemical modification (e.g. displacement of the chloride ligands with the donor solvent). The ^{1}H NMR of **2c** (acetone derivative) gives one set of signals for the 2,2'-bipyridine ligand and two signals for the aminal methyl units. As there are only two possible isomers (*cis*- or *trans*-oid isomers generated by the axial chloride ligand) a simplified spectrum is observed, with two methyl signals arising from *cis*- or *trans*-oid conformation with respect to the axial chloride ligand.

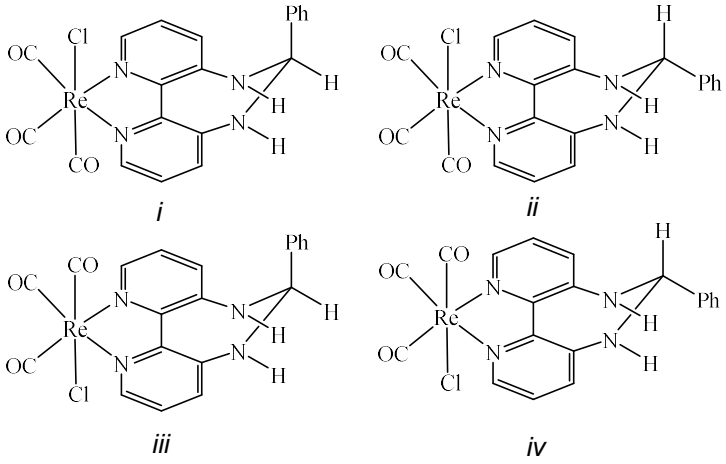

Fig. 2 Structures of the four possible isomers of **2d**.

The advantage of a fluorescent probe of the type of complex **1** is that the metal-to-ligand charge-transfer (MLCT) excited state is likely to be localized on the bipyridine ligand and consequently electronically influenced by alterations in the periphery of the ligand. Therefore, we anticipated that reactions of the 3,3′-diamino group with aldehydes and ketones would modulate the emission properties of the Re(I) complex.

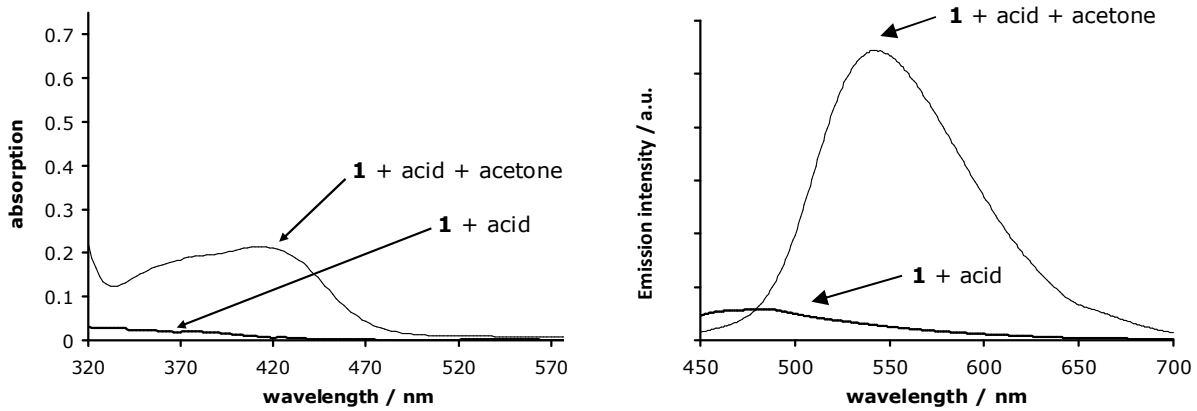

Fig. 3 'In cuvette' spectroscopic analysis of a slight excess of acetone addition to **1**, in the presence of acid. Left: UV-vis. absorption spectra**.** Right: Emission spectra (λ_{ex} = 420 nm). All spectra recorded in water (10^{-5}M).

Initially, luminescence measurements were conducted on the purified complexes. Although **1** itself is not highly soluble in water it was encouraged into solution by dissolving in a drop of methanol and then diluting with water so that the resultant solution was >95% aqueous. Complex **1** was weakly emissive in aqueous solution whereas the corresponding cyclized derivative (**2c**) was strongly fluorescent at 540 nm following excitation at 420 nm. Having assessed the photophysical properties of the purified complexes the *in situ*, *in cuvette* solution state responsiveness of **1** was assessed by both UV-visible absorption and luminescence studies. The electronic spectrum of **1** showed a very weak absorption in the visible region which is likely to be associated with MLCT transitions. This band was not altered upon addition of acid and therefore precludes significant N-lone pair participation. A drop of acetone was then added to the cuvette resulting in the immediate formation of a yellow coloured solution, which deepened in colour over the duration of 5 minutes. This colourimetric response to acetone is shown in Figure 3, which compares the absorption profile before and after the addition of acetone. It is clear that the absorption band responsible for the visible colour change is the broad transition at ~ 450 nm, which is both more intense and red-shifted in comparison to **1**. This dramatic change in optical properties is probably a consequence of the change of the torsion angle of the bipyridine ligand. In the diamine precursor **1** the two pyridine units adopt a non-planar conformation due to the unfavourable steric interactions between the 3,3'-diamino substituents. However, upon reaction with aldehydes and ketones the ligand becomes more planar (NCCN torsion angle reduced to < 1.5 deg) allowing a more conjugated π system and thus enhancing the energetic accessibility of a bipyridine π^* orbital. UV-visible absorption spectra were also obtained on **1** and the four compounds (**2a** – **2d**) in MeCN (10^{-5} M). Firstly, complex **1** revealed a composite of bands between 250-450 nm, wherein intra-ligand based transitions are expected to dominate at higher energies. In common with other rhenium(I) diimine complexes of this type there is likely to be a spin allowed MLCT based transition in the lower energy region of the spectrum, which we tentatively assign to the weaker shoulder feature at 437 nm. Upon reaction with the various aldehyde and ketone substrates, the absorption spectra again show common features. Most notably, a bathochromic shift of a strong (ε ~ 10000) band to 411-424 nm, which may be indicative of a ligand-based absorption that is likely to be superimposed upon the expected ^{1}MLCT band.

Preliminary DFT calculations are consistent with this. Geometry optimisations of the diamine precursor **1** and both *cis*- and *trans-oid* isomers of the cyclised derivative **2c** show the expected reductions in py-py interannular dihedral angle on cyclisation and in each case the HOMO and LUMO show significant metal ($d_{xz/yz}$) and ligand (π^*) contributions respectively (Fig. 4). Furthermore, estimated vertical transition energies to the bipy-centered excited state undergo a red shift of *ca.* 50 nm on going from **1** to the *cis*- and *trans-oid* isomers of the cyclised derivative **2c**.

Luminescence studies revealed a 'switching on' of an intense emission band at 540 nm (as observed for the purified cyclized complex **2c**), following excitation λ_{ex} = 420 nm (Fig. 3). The lifetime of this band was determined as < 1ns suggesting that there may be a significant LC contribution to the ^{3}MLCT excited state or a quenching mechanism occurring such as electron transfer from the bis-aminal lone pairs.

Having established the '*in cuvette*' reaction chemistry of **1** with acetone, a comparative study was conducted with acetaldehyde as the analyte. In this case reaction appeared to be very rapid (addition resulting in an immediate colour change), and did not require the addition of acid to give the cyclized species **2a**. As in the case of acetone, the luminescence studies showed a very large intensity increase in an emission peak at 540 nm, which is reasonable given the structural similarity to **2a**. Consequently, we assessed several ketones and aldehydes of various structural forms. The luminescence studies were in agreement with the structural analysis and an electronically deactivated ketone such as 4-bromoacetophenone was found to be unreactive even in the presence of acid. Benzaldehyde was reactive in the presence of acid giving **2d**, generating the typically yellow solution which was highly fluorescent at 525 nm

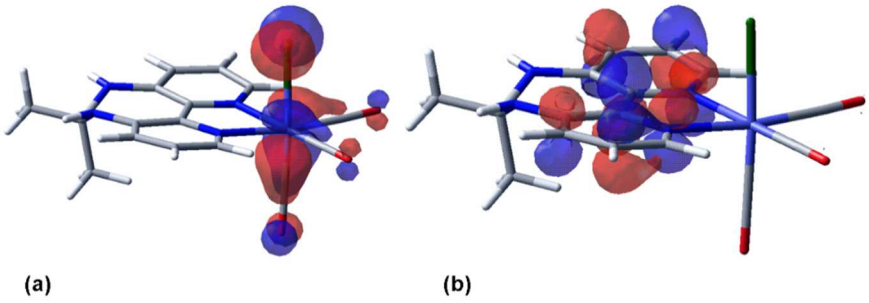

Fig. 4 Surface plots of the (a) HOMO (-5.307 eV) and (b) LUMO (-2.377 eV) for *trans-oid* **2c**.

In summary we have demonstrated how the spectroscopic properties of a Re(I) complex of 3,3′-diamino-2,2′-bipyridine can be modified by the addition of ketones and aldehydes in aqueous solution. Furthermore, the selectivity can be modulated by varying the *p*H and initial studies suggest that aldehydes of different structural form can be discriminated upon by analysis of the emission wavelength.

Experimental.

All reactions were carried out in air and all chemicals and solvents were reagent grade and used without further purification.

Synthesis of **1:** A suspension of 3,3′-diamino-2,2′-bipyridine (0.10 g, 0.54 mmol) and pentacarbonylchlororhenium(I) (0.19 g, 0.54 mmol) was allowed to reflux in chloroform (20 ml) for 8 hrs. After which time the solution was cooled and filtered to give (**1**) as a pale yellow solid (0.11g, 42%).[18] ^{1}H NMR (500 MHz, $(CD_3)_2SO$) δ_H 8.38 (dd, *J* = 5.0, 1.2 Hz, 2H, py), 7.58 (dd, *J* = 8.5, 1.2 Hz, 2H, py), 7.40 (dd, *J* = 8.5, 5.0 Hz, 2H, py), 6.19 (s, 4H, NH_2); ^{13}C (240 MHz, $(CD_3)_2SO$) 199.10 (C=O), 191.99 (C=O), 144.0 (py, quaternary), 142.35 (py, CH), 139.96, (py, quaternary), 128.30 (py, CH), 125.81 (py CH); IR (ATR, νCO) 2017, 1910 and 1863 cm^{-1}); ESI-MS: *m/z* 457 [M-Cl]$^+$.

Reaction of **1** with aldehydes and ketones.

In a typical experiment a small vial was charged with **1** (5 mg, 0.010 mmol) and CH_3CN (0.7 ml), to this was added both benzaldehyde (1 mg, 0.010 mmol) and a catalytic amount of (+/-)-10-camphorsulfonic acid (≈1.0 mg, 3.8x10^{-3} mmol) and the spectra recorded. Concentration and cooling of the CH_3CN solution gave **2d** as a dark yellow solid which was isolated by filtration (3 mg, 51%). ^{1}H NMR (400 MHz, $(CD_3)_2SO$) δ 8.48 (dd, *J* = 5.0, 0.7 Hz, 2H)^a, 8.46 (dd, *J* = 5.0, 0.7 Hz, 2H)^b, 7.83 (d, *J* = 2.6 Hz, 2H, -NH)^a, 7.75 (d, *J* = 2.3 Hz, 2H, NH)^b, 7.71 (m, overlapping)^c, 7.57-7.45 (m, overlapping)^c, 7.30 (dd, *J* = 8.5, 5.1 Hz, 2H)^b, 7.27 (dd, *J* = 8.45, 5.1 Hz, 2H)^a, 5.27 (t, *J* = 2.3 Hz, 1H)^b, 5.16 (t, *J* = 2.6 Hz, 1H)^a. ^{a} corresponds to the minor isomer, ^{b} corresponds to the major isomer (in both cases the integration has been normalised for each particular isomer). ^{c} overlapping peaks corresponding to both isomers; IR (ATR, υCO) 2014, 1911, 1856; ESI-MS: *m/z* 545 [M-Cl$^-$].

2a (acetylaldeyde derivative). Isolated by column chromatography (silica, 10% MeOH in CH_2Cl_2), (3.7 mg, 71%). ^{1}H NMR (400 MHz, CD_3CN) δ 8.50 (dd, *J* = 5.1, 1.2 Hz, 2H), 8.49 (dd, *J* = 5.4, 1.2 Hz, 2H), 7.35 (dd, *J* = 8.4, 1.2 Hz, 2H), 7.36 (dd, *J* = 8.4, 1.2 Hz, 2H), 7.16 (dd, *J* = 8.4, 5.1 Hz, 2H), 7.12 (dd, *J* = 8.4, 5.1 Hz, 2H), 6.01 (br s, 4H), 4.39 (m, 1H), 4.33 (m, 1H), 1.56 (d, *J* = 6.2 Hz, 3H), 1.54 (d, *J* = 6.2 Hz, 3H). IR (ATR, υCO) 2015, 1884, 1847sh cm^{-1}). ESI-MS: *m/z* 541 [M + Na$^+$].

2b (4-nitrobenzaldehyde derivative). Precipitated directly from CH_3CN solution as yellow crystals (5 mg, 80%); ^{1}H NMR (400 MHz, $(CD_3)_2SO$) δ 8.48 (m, *overlapping* 4H, py), 8.31 (d, *J* = 8.2 Hz, 4H, Ar), 8.01 (d, *J* = 3.2 Hz, 2H, NH), 7.95 (d, *J* = 3.1 Hz, 2H, NH), 7.79 (d, *J* = 8.9 Hz, 2H, Ar), 7.76 (d, *J* = 8.8 Hz, 2H, Ar), 7.67 (m, *overlapping* 4H, py), 7.33 (dd, *J* = 4.1, 1.6, 2H, py), 7.31 (dd, *J* = 4.0, 1.7 Hz, 2H, py), 5.55 (t, *J* = 3.1 Hz, 1H, $(NH)_2PhCH$), 5.47 (t, *J* = 3.2 Hz, 1H, $(NH)_2PhCH$); IR (ATR, υCO) 2026, 1920, 1858sh cm^{-1}). ESI-MS: *m/z* 589 [M-Cl$^-$].

2c (acetone derivative). Isolated by column chromatography (silica, 10% MeOH in CH_2Cl_2), (4 mg, 75%). ^{1}H NMR (400 MHz, $(CD_3)_2SO$) δ 8.44 (dd, *J* = 5.0, 1.3 Hz, 2H), 7.54 (dd, *J* = 8.5, 1.3 Hz, 2H), 7.36 (s, 2H, NH), 7.29 (dd, *J* = 8.5, 5.0 Hz, 2H), 1.52 (s, 3H), 1.42 (s, 3H). ^{13}C (240 MHz, $(CD_3)_2SO$) 199.16 (C=O), 192.10 (C=O), 145.63 (py, quaternary), 143.94 (py, CH), 140.91, (py, quaternary), 129.45 (py, CH), 125.45 (py CH), 65.91 ($C(CH_3)_2$), 28.59 ($C(CH_3)_2$), 27.08 ($C(CH_3)_2$); IR (ATR, υCO) 2013, 1891sh, 1875 cm^{-1}); ESI-MS: *m/z* 497 [M-Cl$^-$].

Crystallographic Data.

Crystals of **2d** suitable for analysis by X-ray analysis were obtained as follows: To a solution of **1** (≈ 3 mgs) in MeCN (2 mls) was added an excess of benzaldehyde and a catalytic amount of (+/-)-10-camphorsulfonic acid. The reaction was then gently heated and the hot solution filtered through a plug of cotton wool. The reaction was then allowed to evaporate slowly in the dark. After 24 hrs the solution had concentrated and small dark yellow crystals had formed. Crystal data for **2d** $C_{20}H_{14}ClN_4O_3Re$: M = 580, monoclinic *C2/c*, a = 25.5636(6), b = 11.5038(3), c = 14.5909(3) Å, β = 119.5030(10), V = 3734.47(16) Å^3, Z = 8, $\rho_{(calc)}$ = 2.063 Mgm^{-3}, F(000) = 2224, crystal dimensions 0.15 x 0.14 x 0.12 mm, μ(Mo-κ_α) = 6.682 mm^{-1}, T = 150(2) K. A total of 19086 reflections were measured in the range 2.803 ≤ θ ≤ 33.187° (*hkl* range indices: -39 ≤ h ≤ 39, -14 ≤ k ≤ 17, -22 ≤ l ≤ 22), 7108 unique reflections (R_{int} = 0.0194). The structure was refined on F^2 to R_w = 0.0512, R = 0.0257 (6526 reflections with I>2σ(I)) and *GOF* = 1.152 on F^2 for 262 refined parameters, largest difference peak and hole 2.188 and -1.824 eÅ^{-3}.

Computational details.

All DFT calculations were performed using the Jaguar program package. The calculations were implemented at the B3LYP level of theory,[23] with standard 6-31G* basis sets on all atoms except the Re centres, for which the Jaguar triple-ζ form of the standard Los Alamos ECP basis set (LACV3P*) was used. Solution-phase ground- and excited-state energies were obtained using restricted-open and unrestricted DFT respectively. Solvent effects were simulated using the Poisson-Boltzmann continuum solvent model as implemented in the Jaguar program. Vertical transition energies for the MLCT bands in complexes **1** and *cis*- and *trans-oid* **2c** were estimated from the difference in (single-point) energy between the ground and first excited (triplet) states.

Acknowledgement. The authors would like to thank the Universities of Huddersfield, Cardiff and Bristol. We also acknowledge EPSRC for financial support.

Notes and references

1 Albrecht M, Lutz M, Spek AL and van Koten G. *Nature* 2000; 406: 970.

2 Vickery JC, Olmstead MM, Fung EY and Balch AL. *Angew Chem Int Ed Engl* 1997; 36: 1179.

3 Albrecht M, Gossage RA, Lutz M, Spek AL and van Koten G. *Chem Eur J* 2000: 1431.

4 Buss CE, Anderson CE, Pomije MK, Lutz CM, Britton D and Mann KR. *J Am Chem Soc* 1998; 120: 7783.

5 Grate JW, Moore LK, Janzen DE, Veltkamp DJ, Kaganove S, Drew SM and Mann KR. *Chem Mater* 2002; 14: 1058.

6 Buss CE and Mann KR. *J Am Chem Soc* 2002; 124: 1031.

7 Grove LJ, Rennekamp JM, Jude H and Connick WB. *J. Am Chem Soc* 2004; 125: 1594.

8 Wadas TJ, Wang QM, Kim YJ, Flaschenreim C, Blanton TN and Eisenberg R. *J Am Chem Soc* 2004; 126: 16841.

9 Kato M, Omura A. Toshikawa A. Kishi S and Sugimoto Y. *Angew Chem Int Ed* 2002; 41: 3183.

10 Lu W, Chan MCW, Cheung K-K and Che C-M. *Organometallics* 2001; 20: 22477.

11 Adnan Mansour M, Connick WB, Lachicotte RJ, Gysling HJ and Eisenberg R. *J Am Chem Soc* 1998; 120: 1329.

12 Yam VW-W, Chan C-L, Li C-K and Wong KM-C, *Coord Chem Rev* 2001; 216: 173.

13 Lefebvre J. Batchelor RJ and Leznoff DB. *J Am Chem Soc.* 2004; 126: 16117.

14 Bariain C, Matias IR, Romero I, Garrido J and Laguna M. *Appl Phys Lett* 2000; 77: 2274.

15 Bariain C, Matias IR, Fdez-Valdivielso C, Elosua C, Luquin A, Garrido J and Laguna M. *Sensors and Actuators: B* 2005; 108: 535.

16 Rice CR, Onions S, Vidal N, Wallis JD, Senna MC, Pilkington M and Stoeckli-Evans H. *Eur J Inorg Chem* 2002; 1985.

17 X-ray crystallography data for 2d has been deposited with the Cambridge Crystallographic data Centre CCDC 615248.

18 Bullock S, Hallett AJ, Harding LP, Higginson JJ, Piela SAF, Pope SJA and Rice CR. *Dalton Trans* 2012; 41: 14690.

19 Clegg OR, Harding LP, Miller JW and Rice CR. *Acta Cryst* 2013; E69: m526.

21 Clegg OR, Harding LP, Miller JW and Rice CR. *Acta Cryst.,* 2013; E69: m527.

22 The phenyl group on the diaza-heterocycle is in the axial environment.

23 Becke ADJ. *Chem Phys* 1993; 98: 5648.

Electronic Supplementary Information.

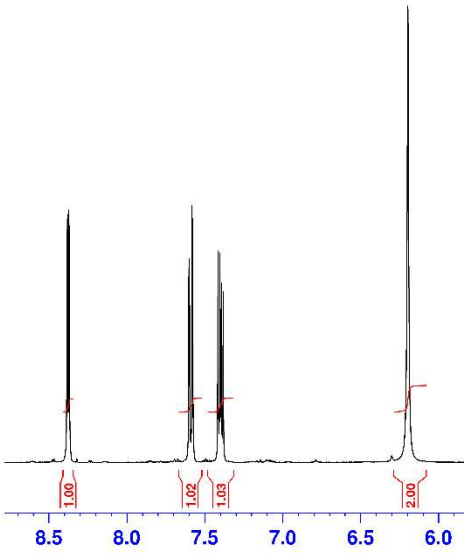

Figure 1. ^{1}H NMR (d^{6}-dmso) of the aromatic region of Re(I) complex **1**.

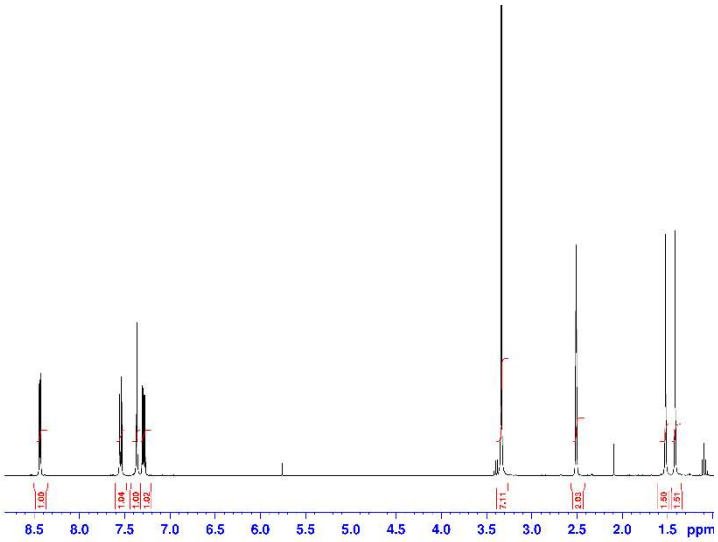

Figure 2. ^{1}H NMR (d^{6}-dmso) of the Re(I) complex **2c**.

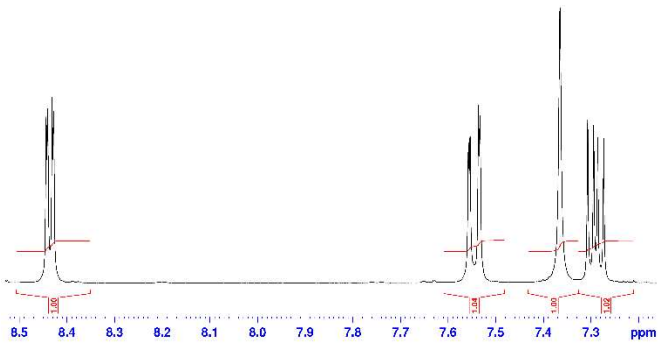

Figure 3. ^{1}H NMR (d^{6}-dmso) of the aromatic region of the Re(I) complex **2c**.

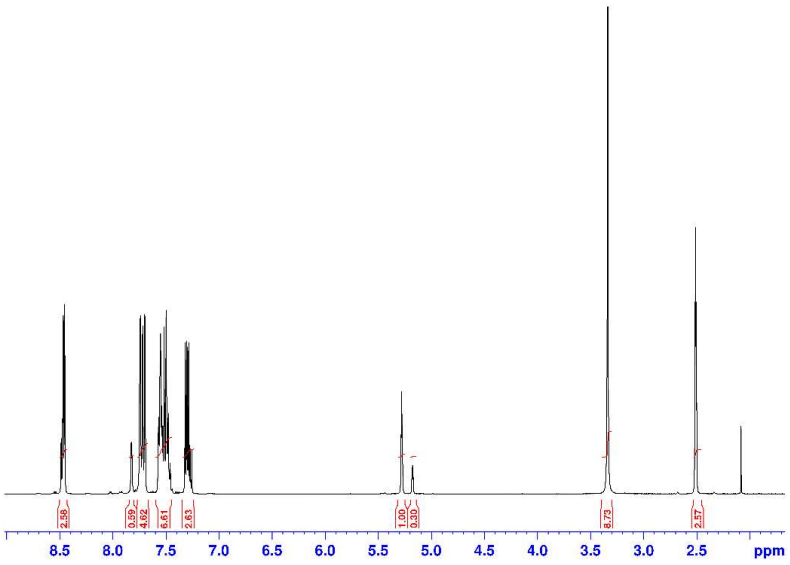

Figure 4. ^{1}H NMR (d^{6}-dmso) of the Re(I) complex **2d**. Showing both the major and minor isomer component.

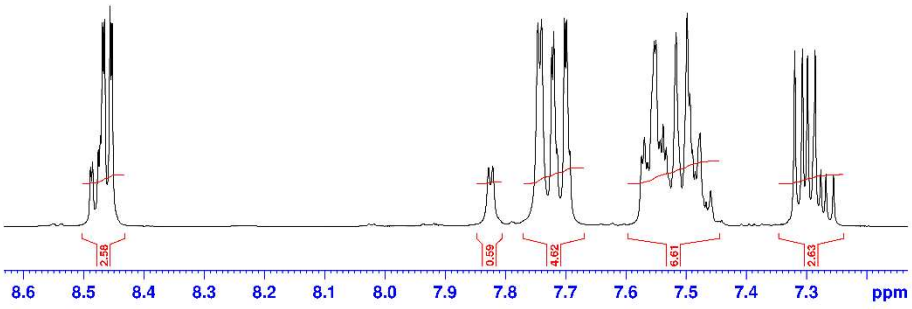

Figure 5. ^{1}H NMR (d^{6}-dmso) of the aromatic region of the Re(I) complex **2d**.

Figure 6. Variable temperature ^{1}H NMR (d^{6}-dmso) of the aromatic region of Re(I) complex **2b**.

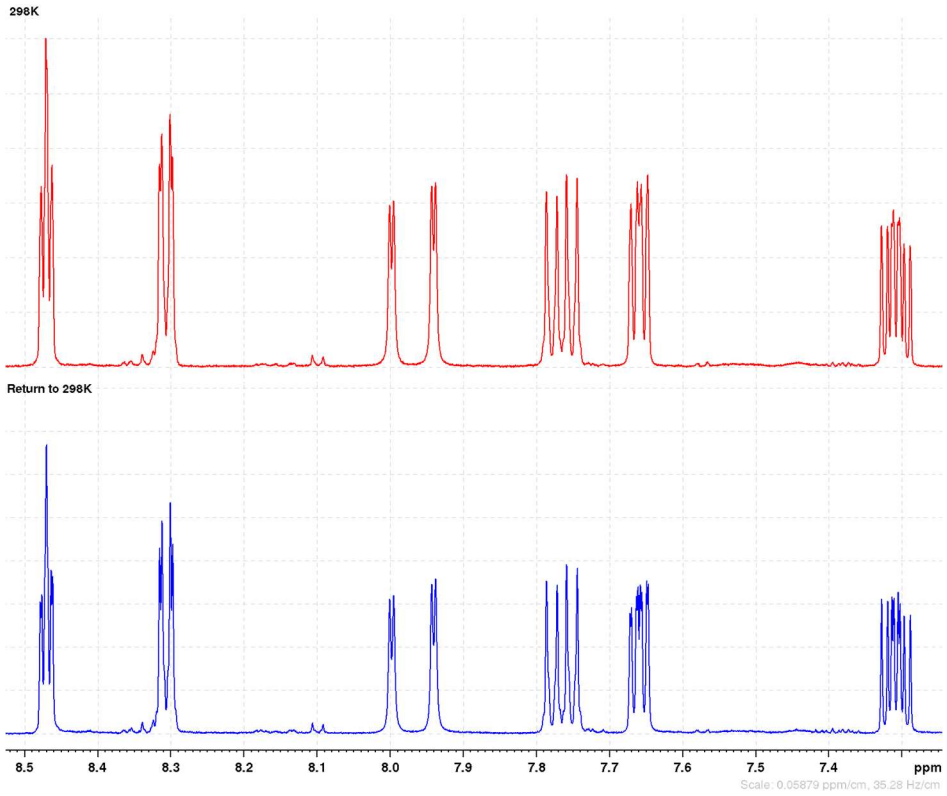

Figure 7. ^{1}H NMR (d^{6}-dmso) of the aromatic region of Re(I) complex **2b**; before heating (top) and after heating and returning to 295K (bottom).

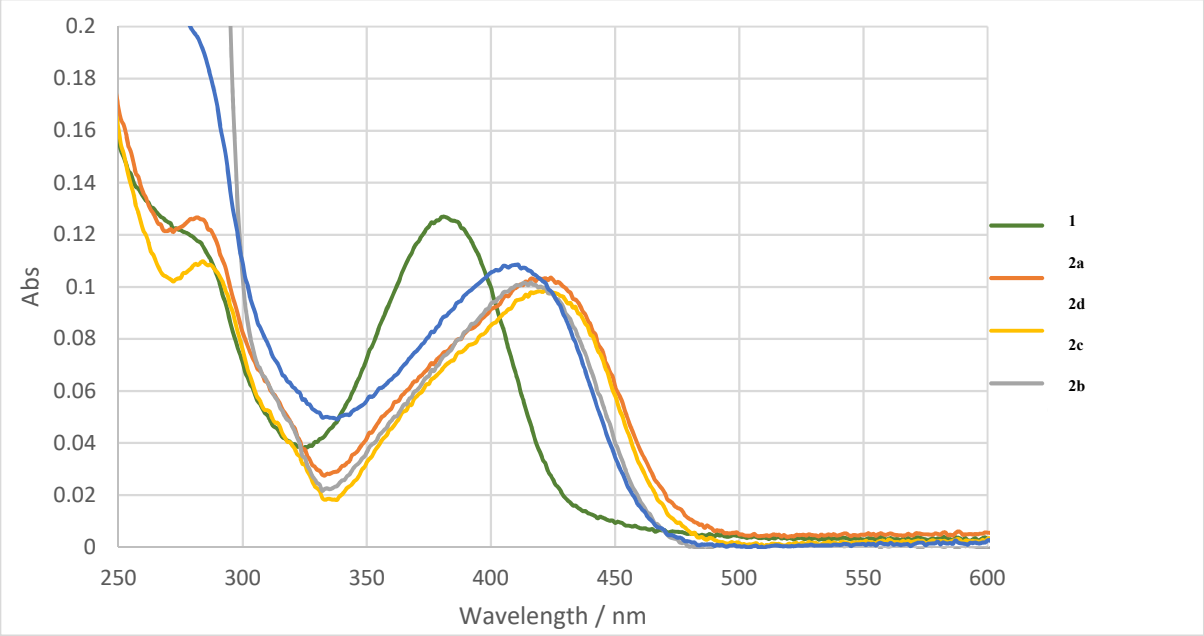

Figure 8. UV-Vis (10^{-4}M, MeCN) of Re(I) complexes **1** and **2a-2d.**

Compound	Absorption wavelength / nm (molar absorption coefficient / $M^{-1}cm^{-1}$)
1	281 (12000), 381 (13000) , 437 sh (2000)
2a	283 (12000), 424 (10000)
2b	282 sh (20000), 318 sh (7000), 411 (11000)
2c	283 (11000), 313 sh (5000), 422 sh (10000)
2d	281 (45000), 289 sh (38000), 311 sh (5000), 416 (10000)

Table 1. Tabulated data of the UV-visible spectra of complex **1** and **2a** – **2d** (10^{-5}M, MeCN).

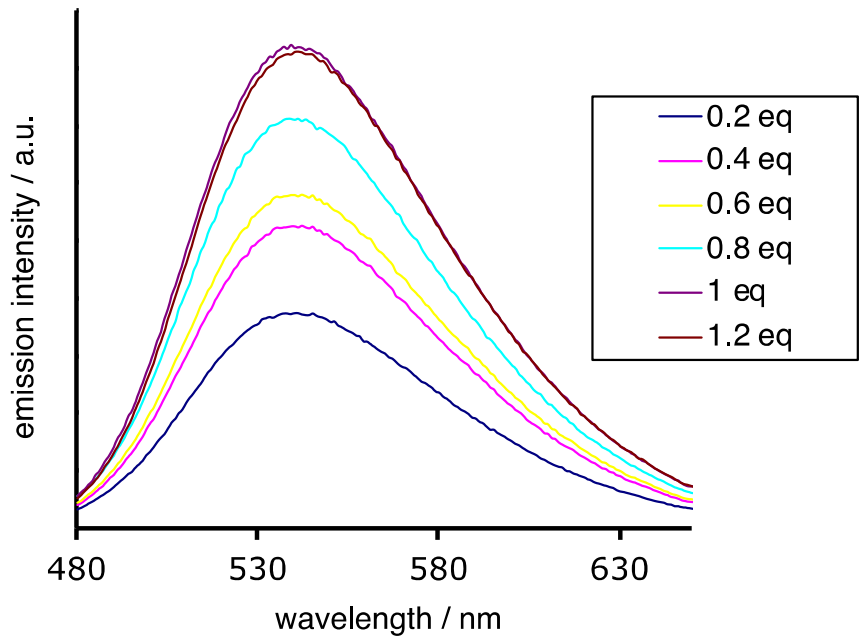

Figure 9. 'In cuvette' UV-vis. absorption spectra analysis of acetone addition to **1**.

Bond lengths (Å) and angles (˚) and esds (in brackets (for the solid-state crystal structure of **2d** $C_{20}H_{14}ClN_4O_3Re$: M = 580, monoclinic *C2/c*, a = 25.5636(6), b = 11.5038(3), c = 14.5909(3) Å, β = 119.5030(10), V = 3734.47(16) Å^3.

Re1 C1 1.913(3)

Re1 C3 1.919(3)

Re1 C2 1.920(3)

Re1 N2 2.148(2)

Re1 N1 2.160(2)

Re1 Cl1 2.5048(6)

N1 C8 1.333(3)

N1 C4 1.374(3)

N2 C13 1.336(3)

N2 C9 1.369(3)

N3 C10 1.358(3)

N3 C14 1.446(3)

N4 C5 1.360(3)

N4 C14 1.450(3)

O1 C1 1.131(4)

O2 C2 1.154(4)

O3 C3 1.153(4)

C4 C5 1.412(3)

C4 C9 1.484(3)

C5 C6 1.405(3)

C6 C7 1.368(3)

C6 H6 0.9500

C7 C8 1.386(4)

C9 C10 1.413(3)

C10 C11 1.401(4)

C11 C12 1.372(4)

C12 C13 1.378(4)

C14 C15 1.503(3)

C15 C20 1.390(4)

C15 C16 1.398(4)

C16 C17 1.394(4)

C17 C18 1.373(5)

C18 C19 1.385(5)

C19 C20 1.389(4)

C1 Re1 C3 87.44(12)

C1 Re1 C2 88.40(14)

C3 Re1 C2 89.33(14)

C1 Re1 N2 95.41(12)

C3 Re1 N2 98.90(11)

C2 Re1 N2 171.06(11)

C1 Re1 N1 92.80(10)

C3 Re1 N1 172.87(11)

C2 Re1 N1 97.79(11)

N2 Re1 N1 73.98(8)

C1 Re1 Cl1 177.61(10)

C3 Re1 Cl1 93.31(8)

C2 Re1 Cl1 93.88(9)

N2 Re1 Cl1 82.23(6)

N1 Re1 Cl1 86.17(5)

C8 N1 C4 120.8(2)

C8 N1 Re1 121.25(16)

C4 N1 Re1 117.91(15)

C13 N2 C9 121.4(2)

C13 N2 Re1 119.65(18)

C9 N2 Re1 118.69(17)

C10 N3 C14 120.7(2)

C5 N4 C14 121.1(2)

O1 C1 Re1 177.5(3)

O2 C2 Re1 177.1(3)

O3 C3 Re1 177.2(3)

N1 C4 C5 118.7(2)

N1 C4 C9 113.84(19)

C5 C4 C9 127.1(2)

N4 C5 C6 117.8(2)

N4 C5 C4 123.5(2)

C6 C5 C4 118.7(2)

C7 C6 C5 120.7(2)

C6 C7 C8 118.2(2)

N1 C8 C7 122.5(2)

N2 C9 C10 118.4(2)

N2 C9 C4 113.8(2)

C10 C9 C4 127.4(2)

N3 C10 C11 117.4(2)

N3 C10 C9 124.1(2)

C11 C10 C9 118.5(2)

C12 C11 C10 120.4(3)

C11 C12 C13 118.7(3)

N2 C13 C12 121.7(2)

N3 C14 N4 110.5(2)

N3 C14 C15 110.6(2)

N4 C14 C15 109.9(2)

C20 C15 C16 119.4(2)

C20 C15 C14 120.1(2)

C16 C15 C14 120.5(2)

C17 C16 C15 119.7(3)

C18 C17 C16 120.5(3)

C17 C18 C19 120.1(3)

C18 C19 C20 120.1(3)

C19 C20 C15 120.2(3)